

## Forced resonant second-order interaction between damped internal waves

By A. D. MCEWAN

C.S.I.R.O. Division of Atmospheric Physics, Aspendale, Victoria, Australia

D. W. MANDER AND R. K. SMITH†

Department of Mathematics, Monash University, Clayton, Victoria, Australia

(Received 3 November 1971 and in revised form 6 June 1972)

A theoretical and experimental study is made of the second-order resonant interaction between triads of linearly damped waves, one common member of which is continuously forced. In the case of a single triad, if the forced wave exceeds a *critical amplitude* defined by properties of the triad members, energy proceeds irreversibly to the other two waves. A stable limit state is reached where all power in excess of that required to sustain a critical amplitude in the forced wave is transferred to the other waves, which also reach steady terminal amplitudes.

It is shown that when two or more triads are simultaneously at resonance the only stable limit state is one wherein the forced wave has fallen to the lowest critical amplitude, and the only other two waves remaining are those of the triad possessing this critical amplitude. Regardless of their initial amplitudes, all other waves not externally forced ultimately disappear.

The theory is applied to the interaction of standing internal gravity waves in a linearly stratified liquid. The experiments described here quantitatively confirm the major predictions.

---

### 1. Introduction

A recent paper (McEwan 1971, henceforth denoted by I) describes experiments to observe the degeneration of continuously forced standing internal gravity waves in a rectangular tank of stably stratified liquid. A single wave was forced at resonance by means of a paddle forming one end of the tank,‡ and it was found that, after a period of time, if the wave was above a certain critical amplitude it suffered an irreversible distortion of form.

It was shown that this degeneration process proceeds by the growth, from a subliminal level, of pairs of free wave modes forming triads in resonant second-order interaction with the original wave. These grow until they have substantially de-energized the original wave. Possible free modes between rectangular boundaries in two dimensions are doubly (countably) infinite in number, but the number of triads participating in resonant interaction for a given geometry

† Present address: Department of Applied Mathematics, University of Edinburgh.

‡ In fact all the odd harmonics as well as the fundamental wave were forced, but the former had insignificant amplitudes.

is singly infinite. If one of the modes is *specified*, exactly resonant interaction is possible only for particular geometries and with a specific pair of triad partners, except in certain special cases.

Theoretical predictions of the critical amplitude of the forced wave (below which degenerate modes could not be sustained) and its dependency on viscous dissipation were accurately confirmed by experiment, but supercritical behaviour was not investigated quantitatively.

Previous theoretical analyses of the phenomenon of resonant interaction between waves† have been concerned mainly with non-dissipative systems, though McGoldrick (1965) gave appropriate solutions to the interaction equations when linear attenuation terms are included. Davis & Acrivos (1967) also considered damping effects, and more recently the effects of viscosity have been examined by McGoldrick (1970) for a case of second-harmonic resonance (between a fundamental mode and its second harmonic) and by Craik (1971) in relation to a resonant instability mechanism in boundary layers.

In §2 of this paper, we undertake an investigation of the equations for a resonantly interacting triad in which one wave is continuously forced and all three are damped. The theory can be generalized, but is developed here in the context of the experiments reported in I. The theory predicts the existence of equilibrium states in which each of the modes reaches a steady terminal amplitude. In §3, the behaviour of two interacting triads having a single forced mode in common is worked out. Stability of the equilibrium states is investigated in §4. In §5, examples and numerical integrations of the interaction equations are given and comments are made on the observations of I. In §6 further experiments which confirm the salient features of the analysis are described.

## 2. Single-triad interaction

The equations governing damped resonant interactions between triads of standing internal gravity waves with one wave forced at resonance are derived in an appendix. These equations have a general form, incorporating dissipation terms of the form first used by McGoldrick (1965), and variable phase angles as in equations (B 14) of Martin, Simmons & Wunsch (1972). We confine our attention here to a triad of standing waves (denoted by subscripts 1, 2 and 3), in which wave 1 is forced continuously at resonance and all three have a time dependence of the form  $a_j(t) \cos(\omega_j t + \alpha_j(t))$ , with frequency  $\omega_j$ , amplitude  $a_j(t)$  (assumed non-negative) and phase  $\alpha_j(t)$ , which is defined only if  $a_j(t)$  is non-zero. If forcing and damping are weak and comparable in size with the nonlinearity in the system, the amplitudes and phases vary slowly with time, in the sense that

$$\max(|a_j^{-1} da_j/dt|, |d\alpha_j/dt|) \ll \omega_j,$$

and their evolution is determined by the six interaction equations

$$\kappa_1^2 da_1/dt = S_1 a_2 a_3 \cos \eta - T_1 a_1 + F \cos(\gamma - \alpha_1), \quad (2.1)$$

† A list of references was given by Phillips (1966); a lucid elementary introduction to the phenomenon was given by Ball (1964).

$$\kappa_2^2 da_2/dt = S_2 a_3 a_1 \cos \eta - T_2 a_2, \tag{2.2}$$

$$\kappa_3^2 da_3/dt = S_3 a_1 a_2 \cos \eta - T_3 a_3, \tag{2.3}$$

$$\kappa_1^2 a_1 d\alpha_1/dt = -S_1 a_2 a_3 \sin \eta + F \sin (\gamma - \alpha_1), \tag{2.4}$$

$$\kappa_2^2 a_2 d\alpha_2/dt = -S_2 a_3 a_1 \sin \eta, \tag{2.5}$$

$$\kappa_3^2 a_3 d\alpha_3/dt = -S_3 a_1 a_2 \sin \eta. \tag{2.6}$$

Here the interaction coefficients  $S_j$  and damping coefficients  $T_j$  are functions of  $\omega_j$  and of the wavenumbers  $\kappa_j$  of the waves ( $\kappa_j$  and  $\omega_j$  are assumed to satisfy the usual resonance conditions  $\Sigma\omega_j = 0, \Sigma\kappa_j = 0$ ). Also  $\kappa_j = |\kappa_j|, \eta = \alpha_1 + \alpha_2 + \alpha_3, F$  is a constant forcing function which is assumed to be positive and  $\gamma = \gamma(t)$  is a function which allows for the possibility of a *slow* drift in the forcing relative to that of the forced wave.† The assumption that  $F$  is constant is based on linear theory, which predicts a uniform growth rate of any mode forced at resonance.

The forms of  $T_j$  appropriate to the experiments reported in I and those described in this paper are given in (5.1), and the  $S_j$  have the form

$$S_j = S\omega_j \tag{2.7}$$

[as was shown to be the case for general systems by Hasselmann (1966, equation (1.13))]. Here, with the  $a_j$  expressed as stream-function amplitudes, the quantity  $S$  takes the form

$$S = \frac{\Omega^2}{8\omega_1\omega_2\omega_3} (m_r\omega_s - m_s\omega_r) (m_s n_r - m_r n_s) \left( \frac{m_1}{\omega_1} + \frac{m_2}{\omega_2} + \frac{m_3}{\omega_3} \right),$$

where  $m_r$  and  $n_r$  are the horizontal and vertical components of  $\kappa_r, \Omega$  is the uniform Brunt-Väisälä frequency of the liquid and  $r$  and  $s$  assume different integer values selected from 1, 2 and 3. One can show by using the resonance conditions that  $S$  is independent of  $r$  and  $s$  and also that the  $S_j$  cannot all be of one sign.

If  $\gamma$  is a constant, (2.1)–(2.6) admit the following two steady-state solutions (denoted by a subscript  $s$ ):

$$\left. \begin{aligned} a_{1s} &= F/T_1, & a_{2s} &= a_{3s} = 0, \\ \alpha_{1s} &= \gamma, & \alpha_2, \alpha_3 & \text{undefined,} \end{aligned} \right\} \tag{2.8}$$

$$\left. \begin{aligned} a_{1s} &= (T_2 T_3 / S_2 S_3)^{\frac{1}{2}}, \\ a_{2s} &= \left[ \left( T_1 - \frac{F}{a_{1s}} \right) \frac{T_3}{S_3 S_1} \right]^{\frac{1}{2}}, \\ a_{3s} &= \left[ \left( T_1 - \frac{F}{a_{1s}} \right) \frac{T_2}{S_2 S_1} \right]^{\frac{1}{2}}, \\ \alpha_{1s} &= \gamma, & \alpha_{2s} &= q\pi - \gamma - \alpha_{3s}, & \alpha_{3s} & \text{arbitrary,} \end{aligned} \right\} \tag{2.9}$$

where  $q = 1$  or  $0$  according as  $S_1 \geq 0$  and conditions necessary for the existence of (2.9) are

- (i)  $S_2 S_3 > 0$ , implying that  $S_3 S_1 < 0, S_1 S_2 < 0$ ,
- (ii)  $F/T_1 > a_{1s}$ .

† In relation to the experiments, see §6.

The solution (2.9) suggests the possibility of realizing steady, † finite amplitude equilibrium states in which energy is transferred from the forced mode to the free modes by resonant interaction and is simultaneously dissipated by all three modes. In the situation represented by (2.8), no energy transfer occurs and the free modes are not present. Since  $F/T_1$  is the terminal amplitude of a non-interacting wave, condition (ii) above means that the forced mode has to be raised to an amplitude greater than the *critical amplitude*

$$a_c = (T_2 T_3 / S_2 S_3)^{\frac{1}{2}} \quad (2.10)$$

for energy transfer between the waves to be maintained. A result which is at first sight surprising is that, for this supercritical state, the terminal level  $a_{1s}$  of the forced mode is equal to  $a_c$  and therefore independent of  $F$ ; in other words, *all excess energy is transferred to the free waves.*

From (2.7) and condition (i) it readily follows that  $\omega_1$  must be of opposite sign to  $\omega_2$  and  $\omega_3$ . Moreover, since  $\Sigma\omega_j = 0$ ,  $|\omega_1| > \max(|\omega_2|, |\omega_3|)$ . That is, *for the existence of a finite amplitude equilibrium state, the triad member with the highest absolute frequency must be forced.* This triad member, as might be expected, is the one which is unstable in inviscid theory to growth of the other two members (Hasselmann 1967). Our numerical solutions suggest that if the forcing is applied only to either of the lower frequency members the interaction will de-energize the highest frequency member to force the other, and regardless of their initial amplitudes both will ultimately fall to zero leaving only the forced mode.

Although conditions (i) and (ii) are sufficient for the existence of a solution of the type (2.9), evolution to this limiting state requires in addition that  $a_2$  and  $a_3$  are not simultaneously zero. In that case interaction cannot occur, even if  $F/T_1$  is supercritical, and the only equilibrium state to which the system may evolve is (2.8). However, we shall show that with supercritical forcing this equilibrium state is unstable.

A shortcoming of our analysis is our inability as yet to rule out completely the possibility of periodic or other fluctuating solutions to (2.1)–(2.6). (Periodic solutions would correspond to limit cycles in a phase-space representation.) Nevertheless, we conjecture that the equilibrium states (2.8) and (2.9) represent *stable* solutions for subcritical and supercritical forcing respectively. In fact, they appear to be the normal states to which the system evolves. The evolution toward a steady state in the experiments follows closely that predicted by the corresponding numerical solution of the interaction equations and, moreover, we have been unable to find quasi-steady states in *any* numerical integrations of the equations.

† The theory is strictly valid on a time scale  $T \sim 1/(\epsilon\Omega)$ , where  $\epsilon$  is a measure of the size of nonlinear terms in the equations (see appendix). Over much longer times, say  $\sim 1/(\epsilon^2\Omega)$ , tertiary wave interactions arising from cubic nonlinearities may become important. However, if  $\epsilon \ll 1$ , the time scales are well separated and *steady*, implying *steady on the time scale T*, is a meaningful concept.

### 3. Multiple-triad interactions

An exploration of the possible mode interactions shows that, for an arbitrarily chosen tank geometry, there are usually several triads which share the forced mode, satisfy the resonance condition  $\sum_{j=1}^3 \kappa_j = 0$  and come close to satisfying  $\sum_{j=1}^3 \omega_j = 0$ . Indeed, for certain specific geometries two or more such triads may be *exactly resonant*. Examples will be given in the next section. For the present, we seek to establish whether, in the equilibrium state, the component waves of two triads sharing the forced wave may all exist at a finite level. The result may be generalized for greater numbers of simultaneously resonant triads.

If a pair of triads is characterized by wavenumbers  $(\kappa_1, \kappa_2, \kappa_3)$  and  $(\kappa_1, \kappa_4, \kappa_5)$ , the interaction equations are

$$\kappa_1^2 da_1/dt = S_1 a_2 a_3 \cos \eta + S_1^* a_4 a_5 \cos \eta^* - T_1 a_1 + F \cos(\gamma - \alpha_1), \tag{3.1}$$

$$\kappa_2^2 da_2/dt = S_2 a_3 a_1 \cos \eta - T_2 a_2, \tag{3.2}$$

$$\kappa_3^2 da_3/dt = S_3 a_1 a_2 \cos \eta - T_3 a_3, \tag{3.3}$$

$$\kappa_4^2 da_4/dt = S_4 a_5 a_1 \cos \eta^* - T_4 a_4, \tag{3.4}$$

$$\kappa_5^2 da_5/dt = S_5 a_1 a_4 \cos \eta^* - T_5 a_5, \tag{3.5}$$

$$\kappa_1^2 a_1 d\alpha_1/dt = -S_1 a_2 a_3 \sin \eta - S_1^* a_4 a_5 \sin \eta^* + F \sin(\gamma - \alpha_1), \tag{3.6}$$

$$\kappa_2^2 a_2 d\alpha_2/dt = -S_2 a_3 a_1 \sin \eta, \tag{3.7}$$

$$\kappa_3^2 a_3 d\alpha_3/dt = -S_3 a_1 a_2 \sin \eta, \tag{3.8}$$

$$\kappa_4^2 a_4 d\alpha_4/dt = -S_4 a_5 a_1 \sin \eta^*, \tag{3.9}$$

$$\kappa_5^2 a_5 d\alpha_5/dt = -S_5 a_1 a_4 \sin \eta^*, \tag{3.10}$$

where  $\eta^* = \alpha_1 + \alpha_4 + \alpha_5$ ,  $S_1^*$  is the value of  $S_1$  calculated from (2.7) with  $r$  and  $s$  assuming different values selected from the integers 1, 4 and 5, and wave 1 is presumed to have the highest frequency.

If  $\gamma$  is a constant, these equations admit the following steady-state solutions:

$$\left. \begin{aligned} a_{1s} &= F/T_1, \\ a_{2s} &= a_{3s} = a_{4s} = a_{5s} = 0, \\ \alpha_{1s} &= \gamma \text{ with } \alpha_{2s} \dots \alpha_{5s} \text{ undefined;} \end{aligned} \right\} \tag{3.11}$$

$$\left. \begin{aligned} a_{1s} &= \left( \frac{T_2 T_3}{S_2 S_3} \right)^{\frac{1}{2}} = a_c, \text{ say,} \\ a_{2s} &= \left[ \left( T_1 - \frac{F}{a_{1s}} \right) \frac{T_3}{S_3 S_1} \right]^{\frac{1}{2}}, \\ a_{3s} &= \left[ \left( T_1 - \frac{F}{a_1} \right) \frac{T_2}{S_2 S_1} \right]^{\frac{1}{2}}, \\ a_{4s} &= a_{5s} = 0, \\ \alpha_{1s} &= \gamma, \quad \alpha_{2s} = q\pi - \gamma - \alpha_{3s}, \\ \alpha_{3s} &\text{ arbitrary, } \alpha_{4s}, \alpha_{5s} \text{ undefined;} \end{aligned} \right\} \tag{3.12}$$

$$\left. \begin{aligned}
 a_{1s} &= \left( \frac{T_4 T_5}{S_4 S_5} \right)^{\frac{1}{2}} = a_c^* \text{ say,} \\
 a_{2s} &= a_{3s} = 0, \\
 a_{4s} &= \left[ \left( T_1 - \frac{F}{a_{1s}} \right) \frac{T_5}{S_5 S_1} \right]^{\frac{1}{2}}, \\
 a_{5s} &= \left[ \left( T_1 - \frac{F}{a_{1s}} \right) \frac{T_4}{S_4 S_1} \right]^{\frac{1}{2}}, \\
 \alpha_{1s} &= \gamma, \quad \alpha_{2s}, \alpha_{3s} \text{ undefined,} \\
 \alpha_{4s} &= q\pi - \gamma - \alpha_{5s}, \quad \alpha_{5s} \text{ arbitrary,} \\
 q &= 0 \text{ or } 1 \text{ according as } S_1^* \leq 0.
 \end{aligned} \right\} \tag{3.13}$$

As in the previous section, it can be shown that solutions (3.12) and (3.13) are possible only if  $F/T_1$  exceeds the corresponding critical amplitudes  $a_c$  and  $a_c^*$  respectively. Thus, if an equilibrium state is attained, only one triad may persist at a finite level. We shall show that the preferred triad is the one with the smallest critical amplitude.

### 4. Stability of equilibrium states

The substitutions  $a_n = a_{ns} + \eta_n$ ,  $\alpha_n = \alpha_{ns} + \eta_{n+5}$  translate the equilibrium solution to the origin in  $\eta$  co-ordinates. The differential equations then take the form

$$\kappa_i^2 d\eta_i/dt = A_{ij} \eta_j + O(|\eta|^2), \tag{4.1a}$$

$$\kappa_i^2 a_{is} d\eta_{i+5}/dt = B_{ij+5} \eta_{j+5} + O(|\eta|^2), \tag{4.1b}$$

where  $i = 1, \dots, 5$  and

$$(A_{ij}) = \begin{bmatrix} -T_1 & S_1 a_{3s} & S_1 a_{2s} & S_1^* a_{5s} & S_1^* a_{4s} \\ S_2 a_{3s} & -T_2 & S_2 a_{1s} & 0 & 0 \\ S_3 a_{2s} & S_3 a_{1s} & -T_3 & 0 & 0 \\ S_4 a_{5s} & 0 & 0 & -T_4 & S_4 a_{1s} \\ S_5 a_{4s} & 0 & 0 & S_5 a_{1s} & -T_5 \end{bmatrix}$$

and

$$(B_{ij}) = (-1)^{1-i}$$

$$\times \begin{bmatrix} S_1 a_{2s} a_{3s} + S_1^* a_{4s} a_{5s} + (-1)^i F & S_1 a_{2s} a_{3s} & S_1 a_{2s} a_{3s} & S_1^* a_{4s} a_{5s} & S_1^* a_{4s} a_{5s} \\ S_2 a_{3s} a_{1s} & S_2 a_{3s} a_{1s} & S_2 a_{3s} a_{1s} & 0 & 0 \\ S_3 a_{1s} a_{2s} & S_3 a_{1s} a_{2s} & S_3 a_{1s} a_{2s} & 0 & 0 \\ S_4 a_{5s} a_{1s} & 0 & 0 & S_4 a_{5s} a_{1s} & S_4 a_{5s} a_{1s} \\ S_5 a_{1s} a_{4s} & 0 & 0 & S_5 a_{1s} a_{4s} & S_5 a_{1s} a_{4s} \end{bmatrix}.$$

Equations (4.1a) and (4.1b) may be regarded as a single set of ten coupled equations in the ten-dimensional phase space  $\{\eta\}$ , with the first five governing perturbations to the amplitudes of the waves and the rest perturbations to the phases, in the neighbourhood of the equilibrium state. If the perturbations are

small, so that terms of  $O(|\eta|^2)$  can be neglected, the two sets *decouple* and can be studied separately in the appropriate subspace of  $\{\eta\}$ .

The linearized version of (4.1) has solutions of the form

$$\eta_i = c_i e^{\lambda t},$$

where  $\lambda$  is an eigenvalue of the matrix  $(A_{ij})$ . If none of the eigenvalues has a positive real part, then all perturbations in amplitude are *stable*; otherwise they are *unstable*.

Consider first the steady solution (3.11). The characteristic equation for  $(A_{ij})$  is then

$$(T_1 + \lambda) [(T_2 + \lambda)(T_3 + \lambda) - S_2 S_3 F^2 / T_1^2] [(T_4 + \lambda)(T_5 + \lambda) - S_4 S_5 F^2 / T_1^2] = 0$$

and it readily follows that all the roots  $\lambda$  have negative real parts if and only if  $F/T_1 < \min(a_c, a_c^*)$ . Moreover, since  $a_{2s} \dots a_{5s}$  are zero,  $\alpha_{2s} \dots \alpha_{5s}$  are undefined and the linearized form of (4.1 *b*) reduces to a single equation:

$$\kappa_1^2 a_{1s} d\eta_6 / dt = -F\eta_6,$$

whence

$$\eta_6 \propto \exp(-Ft / \kappa_1^2 a_{1s})$$

and perturbations to the phase  $\alpha_{1s}$  are stable. Hence, *the equilibrium solution (3.11) is unstable if  $F/T_1$  exceeds the smallest critical amplitude; otherwise it is stable.*

For the steady solution (3.12), the characteristic equation for the eigenvalues  $\lambda$  of  $(A_{ij})$  is

$$\begin{vmatrix} -(T_1 + \lambda) & S_1 a_{3s} & S_1 a_{2s} & 0 & 0 \\ S_2 a_{3s} & -(T_2 + \lambda) & S_2 a_{1s} & 0 & 0 \\ S_3 a_{2s} & S_3 a_{1s} & -(T_3 + \lambda) & 0 & 0 \\ 0 & 0 & 0 & -(T_4 + \lambda) & S_4 a_{1s} \\ 0 & 0 & 0 & S_5 a_{1s} & -(T_5 + \lambda) \end{vmatrix} = 0. \quad (4.2)$$

After substituting for  $a_{1s}$ ,  $a_{2s}$  and  $a_{3s}$  from (3.12), we see that the cubic factor of the above determinant is

$$\lambda^3 + (T_1 + T_2 + T_3)\lambda^2 + (T_2 + T_3)F\lambda/a_c + T_2 T_3 \left(\frac{F}{a_c} - T_1\right) = 0,$$

and it is evident that all roots have negative real parts if  $F/T_1 > a_c$ . The quadratic factor is

$$(T_4 + \lambda)(T_5 + \lambda) - S_4 S_5 a_c^2 = 0, \quad (4.3)$$

which has roots with negative real parts if and only if  $a_c^2 < T_4 T_5 / S_4 S_5$ , i.e. if  $a_c < a_c^*$ .

Since  $a_{4s}$  and  $a_{5s}$  are both zero,  $\alpha_{4s}$  and  $\alpha_{5s}$  are undefined and the linear system (4.1 *b*) comprises three equations for  $\eta_6$ ,  $\eta_7$  and  $\eta_8$ . The eigenvalues for this system satisfy the cubic equation

$$\lambda(\lambda^2 - \lambda(P + Q - F) - FQ) = 0,$$

where  $P = (-1)^{1-q} S_1 a_{2s} a_{3s}$  and  $Q = (-1)^{1-q} a_{1s} (S_2 a_{3s} + S_3 a_{2s})$ . This equation has roots

$$\lambda = 0, \quad 2\lambda = P + Q - F \pm [(P + Q - F)^2 + 4QF]^{1/2},$$

and the non-zero roots have negative real parts since

$$\text{sgn}(QF) = (-1)^{1-q} \text{sgn}(S_2) = -1$$

and if  $F > T_1 a_{1s}$ ,

$$P - F = (-1)^{1-q} S_1 a_{2s} a_{3s} - F = -T_1 a_{1s} < 0.$$

There is a neutrally stable eigensolution corresponding to the eigenvalue  $\lambda = 0$  and this reflects the degree of arbitrariness between  $\alpha_{2s}$  and  $\alpha_{3s}$ . As the other eigensolutions both decay, no unstable growth of the phase perturbations can occur although a finite jump in  $\alpha_{2s}$  and  $\alpha_{3s}$ , keeping  $\alpha_{2s} + \alpha_{3s} + \gamma = q\pi$ , is theoretically possible.

We conclude, therefore, that, of the two possible equilibrium solutions (3.12) and (3.13), the one which is stable to small disturbances when  $F/T_1 > \max(a_c, a_c^*)$  is the one with the lowest critical amplitude and the other is unstable.

This result may be extended to cover the situation where, say,  $k$  resonant triads are simultaneously present. Theoretical limit states and an  $a_{ck}$  for each additional triad may be defined, but the appropriate additions to the determinant (4.2) only result in the inclusion of quadratic factors

$$(T_{2k} + \lambda)(T_{2k+1} + \lambda) - S_{2k} S_{(2k+1)} a_{1s}^2,$$

in the quadratic factor (4.3). Each quadratic independently has roots with negative real parts only if  $a_{1s}$  is less than the corresponding  $a_{ck}$ .

## 5. Some numerical calculations

### 5.1. Parameter definition

The foregoing analysis may be related directly to the experiments reported in I and to the present experiments, by substitution of calculated values for the controlling parameters. The interaction coefficient  $S_j$  has been defined in (2.7); provided that the container wall boundary layers remain laminar, the dissipation coefficients  $T_j$  are as given in I, viz.

$$T_j = \frac{\omega_j}{R_j} \left[ \left( \frac{H}{B} (mn + n^2)_j + \frac{2H}{L} m_j n_j + 2n_j^2 \right) (2R_j)^{\frac{1}{2}} + H^2 (m^2 + n^2)_j^2 \right], \quad (5.1)$$

where the quantities within the square brackets are boundary-layer and internal-dissipation terms respectively;  $R_j$  is a dissipation parameter or 'Stokes number' defined as  $\omega_j H^2 / \nu$  ( $\nu$  = kinematic viscosity); the container has length  $L$ , breadth  $B$  (normal to the plane of motion) and depth  $H$ . The quantities  $m_j$  and  $n_j$  are related to the horizontal and vertical modal numbers  $M_j$  and  $N_j$  of the waves by

$$m_j = M_j \pi / L, \quad n_j = N_j \pi / L. \quad (5.2)$$

Further reference to waves is made in terms of their modal number ratio, e.g.  $M_2/N_2 = 6/3$ .

The forcing constant  $F$  is defined by the angular displacement  $A \sin(\omega_1 t + \gamma)$  of the fixed wave maker (described in §6.1), and the phase  $\theta$  of the forcing is equal to the phase difference  $(\gamma - \alpha_1)$  between the forced wave ( $j = 1$ ) and the

Forced mode	Triad partners		$ (\omega_2 + \omega_3)/\omega_1 $	$Q_c \times 10^3$ at $R_1 = 10^5$
1/1	4/10	5/9	0.991	—
	5/11	6/12	0.991	—
	5/12	6/11	0.998	—
	6/13	7/14	0.998	—
	6/14	7/13	1.003	—
	7/15	8/16	1.003	—
	8/15	7/16	1.007	—
	etc.			
2/1	1/3	3/2	1.001	32.07
	3/4	5/5	1.000	13.92
	9/11	11/12	0.994	25.55
	9/12	11/11	1.000	58.92
	10/12	12/13	1.005	28.45
3/1	1/2	2/1	1.008	—
	5/5	8/6	1.009	—
	6/6	9/7	0.992	—
	6/7	9/6	1.010	—
	7/8	10/7	0.992	—
	13/12	16/13	1.005	—
	13/13	16/12	1.010	—
	14/13	17/14	0.996	—
	14/14	17/13	1.000	—
	15/15	18/14	0.992	—
4/1	4/5	8/4	1.002	—
	8/8	12/7	1.001	—
	12/10	16/11	0.994	—
	12/11	16/10	1.000	—
5/1	1/1	4/2	0.999†	3.46
	3/3	8/4	0.999†	2.94
	7/7	12/6	0.999†	4.33
	10/8	15/9	0.997	4.53
	10/9	15/8	1.006	5.24
	13/10	18/11	1.004	5.59
	13/11	18/10	1.009	—

† These triads are simultaneously in exact resonance at  $L = 3.094H$ .

TABLE 1. Lowest triads within 1% of resonance frequency:  $L = 3.10H$

wave maker. In ideal conditions,  $\theta = 0$  although in the experiments it was liable to drift over a small range of angles about  $\frac{1}{2}\pi$  (§ 6.1). From I, with  $\phi = \theta + \frac{1}{2}\pi$ ,

$$F = 4\omega_1^2 A \sin \phi / \pi^2 M_1 N_1. \tag{5.3}$$

With the above definitions,  $a$  is in units of stream function  $\psi$ , the field description being

$$\psi_j = a_j \sin m_j x \sin n_j z \cos (\omega_j t + \alpha_j), \tag{5.4}$$

where  $x$  and  $z$  are length and depth co-ordinates measured from the fixed wave maker. The non-dimensional form of  $a_j$ ,

$$Q_j = a_j / \omega_j H^2, \tag{5.5}$$

is preferred in the presentation of the results.

5.2. *Examples of interacting triad groups*

As was mentioned earlier, the nearly resonant triads sharing the forced wave may be numerous for particular geometries. Table 1 lists as a pertinent example the lowest triads whose values of  $|(\omega_2 + \omega_3)|$  differ from  $\omega_1$  by less than 1%, when  $L/H = 3.10$ . For some of these the critical amplitude  $Q_c = a_c/\omega_1 H^2$ , with  $R_1 = 10^5$ , is also given. It is notable that the critical amplitudes do not increase rapidly with unstable modal number. In one tabulated case, three triads sharing the 5/1 forced mode may be simultaneously in exact resonance. Sample calculations were performed on this case.

5.3. *Unstable double-triad interaction without phase variation*

In this first example, the interaction equations (3.1)–(3.5) were numerically integrated with the initial conditions and predicted limit amplitudes (in units of  $Q$ ) as listed in table 2.

Mode $i$	$M/N$	$Q(t=0)$	$Q(t \rightarrow \infty)$	$\alpha(t=0)$	$F/T_1 a_c$
2	3/3	$8 \times 10^{-5}$	$4.195 \times 10^{-3}$	0	} 3.54
3	8/4	$8 \times 10^{-5}$	$1.832 \times 10^{-3}$	0	
1	5/1	0	$2.939 \times 10^{-3}$	0	
4	1/1	0	0	0	} 3.11
5	4/2	$1 \times 10^{-2}$	0	0	

TABLE 2

The tank length is simultaneously resonant for both the (5/1, 3/3, 8/4) and (5/1, 1/1, 4/2) triads, at  $3.09423H$ . Dissipations were chosen to be appropriate to  $R_1 = 10^5$ . The initial amplitudes were chosen both to be relevant to experiments and to illustrate the predictions of §4; the triad (5/1, 3/3, 8/4), though initially weaker, possesses a lower critical amplitude (and hence, higher  $F/T_1 a_c$ , see table 2) than the other triad and ultimately acquires the excess energy supplied to the forced mode.

The initial phases are all zero, and  $\gamma$  is taken to be zero, so that the phase equations (3.6)–(3.10) are superfluous in this example.

Figure 1 presents the integration to 2000 cycles of the forced mode. Up to time (a) mode 4 is energized by the interaction of modes 5 and 1. These settle toward equilibrium values (b), but meanwhile modes 2 and 3 have gradually grown and gradually de-energize mode 1 (region (c)) towards its lower critical level. Modes 4 and 5 can no longer be sustained and gradually decay altogether, while modes 1, 2 and 3 approach their steady terminal values at (d). The conditions in this calculation are realistic for an experiment, and it can be seen that the time scales for attainment of limit states are long, of order  $10^3$  cycles of main mode forcing. Other integrations show that the time scales depend only weakly on the initial amplitudes chosen.

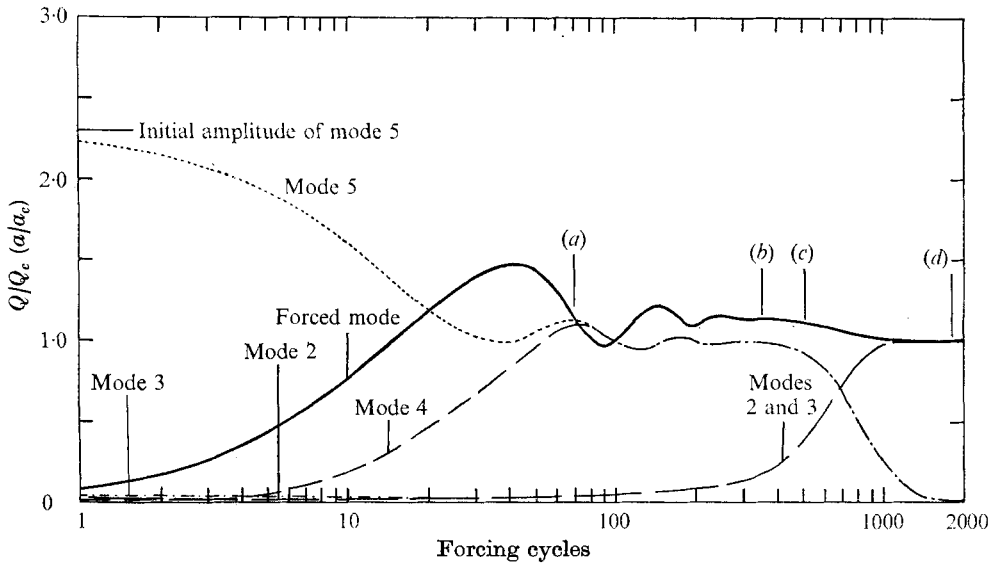


FIGURE 1. Evolution of a resonant interaction with two unstable triads initially present. Amplitudes are presented as fractions of their limit-state values. Initial conditions are given in table 2. The triad (5/1, 3/3, 8/4) possesses a lower critical amplitude than the triad (5/1, 1/1, 4/2).

Mode $i$	$M/N$	$\alpha(t=0)$ (rad)	$Q(t=0)$	$F/T_1 a_c$	$Q(t \rightarrow \infty)$	$\alpha(t \rightarrow \infty)$ (rad)
1	5/1	1	0	3.539	$2.939 \times 10^{-3}$	0
2	3/3	$\frac{1}{2}\pi$	$10^{-3}$	3.539	$4.195 \times 10^{-3}$	+0.530
3	8/4	0	$10^{-3}$	3.539	$1.832 \times 10^{-3}$	-0.530

TABLE 3

#### 5.4. Unstable single-triad interaction with phase variation

As a second example, the interaction equations (2.1)–(2.6) were solved for the same tank geometry and  $R_1$  as in § 5.3 but with initial phases defined, and  $\gamma = 0$ . Conditions are given in table 3.

Solutions are shown in figure 2. The phase of each mode settles rapidly to its limit state with very little overshoot. Oscillation of the amplitudes about the final limit amplitude is protracted over a period ten times as long, about 500 cycles. Most of the phase adjustment occurs before rapid energization of the unstable modes has commenced.

#### 5.5. Relation to previous experiments

The experiments of I were directed mainly towards confirming the occurrence of resonant interaction and in verifying the value of  $a_c$  for a single triad. The observations summarized in table 1 of I do in addition offer partial confirmation of the present predictions. In each case except the first (1/1 mode forcing), the most commonly detected mode has the lowest  $a_c$ . The reason for the appearance

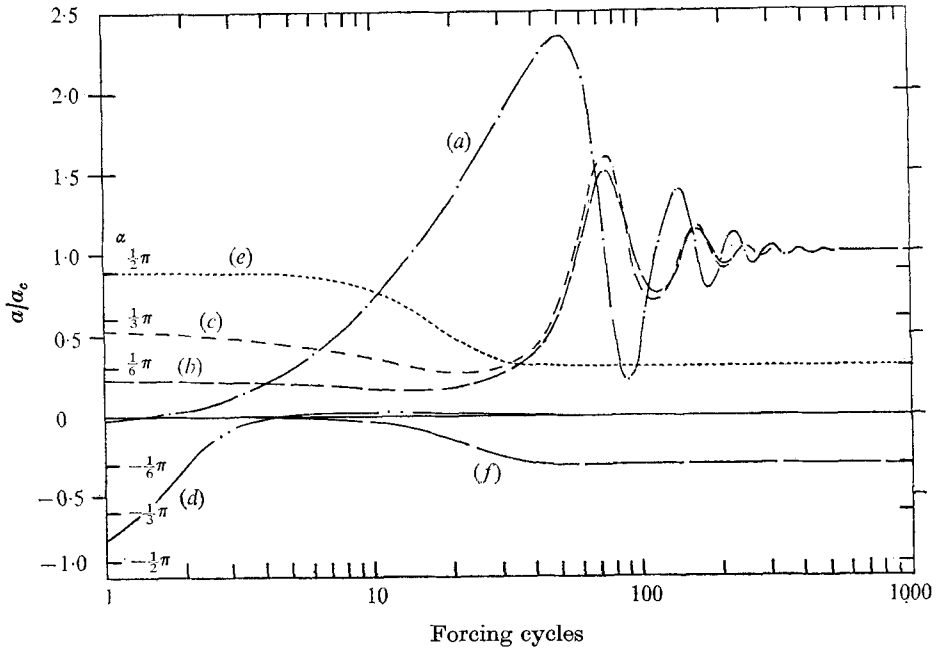


FIGURE 2. Evolution of a single-triad interaction with initial phases prescribed. Conditions are given in table 3. (a) Forced 5/1 mode, (b) 3/3 mode, (c) 8/4 mode, (d)  $\alpha_1$ , (e)  $\alpha_2$ , (f)  $\alpha_3$ . The tank length is  $3.094H$  and forcing is at  $3.539$  times the critical rate.

of different modes when forcing was strong may well have been that these, by virtue of initial transients, had higher initial amplitudes. Subsequent traumatic distortion of the density field would have obscured any subsequent transfer to the more unstable triads.

## 6. Experiments

The apparatus described in I was modified for the present study. Figure 3 is a simplified sketch of the arrangement. The transparent-sided rectangular tank  $1.83$  m long,  $0.228$  m wide and  $0.382$  m deep was filled to a depth of  $0.326$  m with linearly stratified salt solution. A sheet of P.V.C. was laid on the surface to inhibit evaporation and present a nearly rigid boundary. Internal waves were forced within a confined part of the tank by two independently driven wave makers. The first, like that used previously, was a single plane paddle (a), pivoting about a fixed horizontal axis  $16.3$  cm above the bottom and parallel to the ends. This was oscillated through a small arc about its vertical mean position. The other, movable, wave maker (b) could be inserted at any preselected position in the length of the tank, and comprised a pair of plane paddles pivoting about their central horizontal axes,  $8.15$  and  $24.45$  cm above the bottom and normal to the tank sides. The mean position of these paddles was a vertical plane, and they were linked together by pulleys so that, when the upper paddle was oscillated through a small arc, the lower one also moved to produce a deformation of the

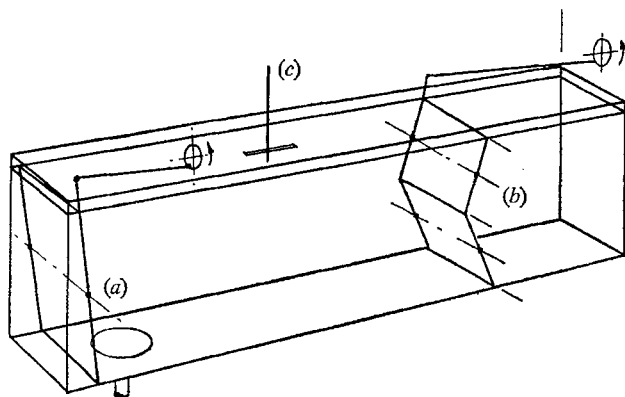


FIGURE 3. Experimental arrangement (diagrammatic).

liquid boundary closely approximating a full wavelength of a triangular wave form. Both wave makers were sealed round their edges with felt, and a sheet of rubber glued to the face of the second one presented a smooth leak-free joint between the two paddles. Each wavemaker was driven from a crank by its own electronically controlled d.c. motor.

The amplitude of forced waves was derived from speed measurements made at one point in the liquid using a thermistor probe (*c*) (described in I) connected in a 'constant-temperature' bridge circuit. Coupled with this was a device for measuring the phase of speed minima relative to the forcing oscillations. Speed and phase were recorded against time.

The thermistor probe, while being a sensitive and accurate means of measuring speeds as low as 1 mm/s, had a time constant (due to encapsulation in a 0.2 mm glass bead and electrically insulating lacquer) of about 1 s. To avoid measurement error it was necessary to calibrate the probe, after each experiment, by oscillating it through measured amounts in a manner closely reproducing the motion field experienced during the previous experiment. To do this would have been impossible if the motion field had contained numerous components of different frequency, and a complicated and expensive procedure of linearization compensation and Fourier analysis would have been required for measurement of component wave amplitudes.

Fortunately, a far simpler procedure could be used to give quantitative verification of the analysis of § 2 in the present experiments. The triad (3/1, 2/1, 1/2) was selected for its simplicity, and the large scale of its modes. The resonance  $L/H$  ratio was 3.208, satisfying (A 7), and the movable wave maker was set to confine this geometry. The probe was located at  $(\frac{1}{2}L, \frac{1}{2}B, \frac{1}{12}H)$ . This is a *nodal* position of horizontal velocity for the 2/1 (and other even) modes, but an *antinode* for the 3/1 and 1/2 modes, which could be forced by the fixed and movable wave makers respectively.

Because of the scale of these latter modes, it was expected that, for the moderate wave amplitudes used, the motion at the probe contained only two dominant collinear horizontal components of different frequency. Reproduction of this

motion was accomplished by disconnecting the wave makers and using their cranks to drive a mechanical linkage which combined two reciprocating components of frequencies  $\omega_1$  and  $\omega_2$  (equal to those of the experiment) and amplitudes  $\beta_1$  and  $\beta_2$  into a horizontal displacement of the probe. The amplitudes could be varied to give a modulated trace on the recorder, resembling part of those obtained during an experiment. Calibration was achieved by using a measurement of the maximum and minimum levels of the *upper* envelope of the thermistor record, representing  $|\omega_1\beta_1 + \omega_2\beta_2|$  and  $|\omega_1\beta_1 - \omega_2\beta_2|$  respectively. Provided that  $|\beta_2\omega_2|$  was less than 80% of  $|\beta_1\omega_1|$  (with  $\omega_1 > \omega_2$ ), the modulation range could be measured and calibrations reproduced to within  $\pm 3\%$ . Graphical interpolation was used to derive the modal amplitudes (figures 4 and 5) from experimental records such as figure 6(a) (plate 1). Spot checks by shadowgraph of particle displacements during experiments confirmed the accuracy to better than 5%.

The presence of additional modes is revealed by the appearance of multiple modulations on the recorder trace. While these were sought for multiple interactions (see § 6.3 below), no quantitative measurements were made from such records.

### 6.1. *Limit-state experiments*

For these experiments the fixed paddle amplitude was preset and the 3/1 mode was forced continuously at resonance. Since a limit state is attainable only when  $|\gamma - \alpha_1| = 0$  (see equation (2.8)), this phase difference was monitored and minimized during a test by continual minute adjustments to the forcing frequency. In relation to the theory this was equivalent to minimizing the time dependency of  $\gamma$ . Variations in  $\gamma$  and compensations occurred in time scales short compared with evolutionary time scales, but as far as possible long-scale variations were averaged out. The 2/1 and 1/2 unstable modes were allowed to grow either spontaneously or with the help of a cycle or so of forcing by the movable wave maker. Only on such occasions was this wave maker used; for the remaining time it was stationary at its mean vertical position.

Forcing was sustained at a constant level until the thermistor output appeared to have stabilized, giving constant levels of maxima and minima in the speed record. In some cases this state was attained only after many hundreds of forcing cycles (q.v. figure 1). Accuracy was limited by the difficulty in sustaining a constant phase for so long a period, and the necessity of subjectively judging when the limit state had been reached.

Figure 4 summarizes the results. The wave amplitudes  $a_1$  and  $a_3$  and the forcing function  $F$  have been normalized by the factors

$$(S_2S_3/T_2T_3)^{\frac{1}{2}}, \quad (S_1S_2/T_1T_2)^{\frac{1}{2}} \quad \text{and} \quad 1/T_1a_c$$

respectively. Each symbol refers to results obtained with a particular filling of the tank (and hence, a specific value of the dissipation parameter  $R_1$ ).

The experimentally determined values of  $a_{1s}$  and  $a_{3s}$  agree with the form predicted by (2.9) quite closely. With supercritical forcing  $a_{1s}$  generally exceeded the predicted  $a_c$  by a few per cent. This was matched by an apparent underestimate in the value of  $F_{1c}$ , though the subsequent growth in  $a_{3s}$  with  $F$  was well followed.

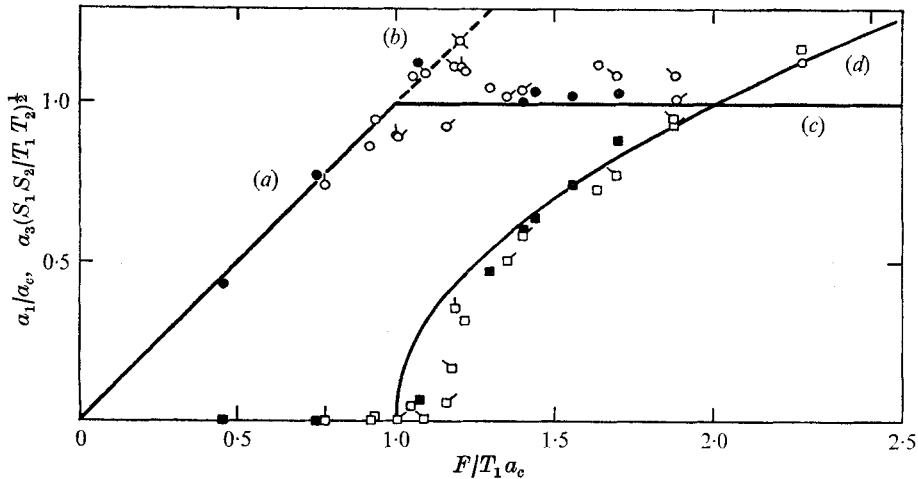


FIGURE 4. Theoretical and experimental limit states compared. (3/1, 2/1, 1/2) triad interaction. (a) Theoretical subcritical 3/1 mode. (b) Supercritical unstable 3/1 mode. (c) Supercritical limit-state 3/1 mode. (d) Supercritical 1/2 mode. Experiments: round symbols refer to the 3/1 forced mode, square symbols to the 1/2 free mode.  $\circ$ ,  $R_1 = 6.10 \times 10^4$ ;  $\bullet$ ,  $7.23 \times 10^4$ ;  $\odot$ ,  $1.01 \times 10^5$ ;  $\ominus$ ,  $1.02 \times 10^5$ ;  $\circ$ ,  $1.08 \times 10^5$ ;  $\text{X}$ ,  $1.08 \times 10^5$  before instability.

In one series, marked by filled symbols, conditions were sustained for exceptionally long periods, and these pains are reflected in the quality of the results. However, slight discrepancies remain, tending to suggest that a small proportion of the energy extracted from  $a_1$  by interaction was not finding its way to  $a_2$  and  $a_3$ , although the theoretical estimates of interaction and dissipation were accurate.

### 6.2. Measurement of an unstable interaction

To test experimentally the amplitude growth equations (2.1)–(2.3) initial amplitudes of each participating mode need to be defined. This was accomplished by oscillating the movable wave maker at the resonant frequency of the 1/2 mode until it had stabilized at a measurable level. Then, simultaneously, this wave maker was disengaged and the fixed wave maker engaged at the (present) 3/1 mode resonant frequency. The 2/1 mode was initially absent, but grew immediately through interaction between the 3/1 and 1/2 modes, and its phase was predetermined by that of the 1/2 mode.

Several such tests were performed, and results of one are compared with the computed evolutionary cycle in figure 5. The computations included both amplitude and phase equations with the measured phase difference  $(\gamma - \alpha_1)$  as a function of  $t$  as an input variable, as well as the values of  $a_1$ ,  $a_2$  and  $a_3$  at  $t = 0$ . Observed values of  $Q_1$  tend to be higher than those predicted and  $Q_3$  lower as the limit state is reached. This is consistent with the limit-state experiments. Agreement is considered to be remarkably good, however, in view of the difficulties experienced in accurately calibrating the highly modulated thermistor probe signal (figure 6(a), plate 1). Computations performed without the phase equations (2.4)–(2.6) gave an almost identical amplitude evolution, indicating insensitivity to the weak phase variations experienced.

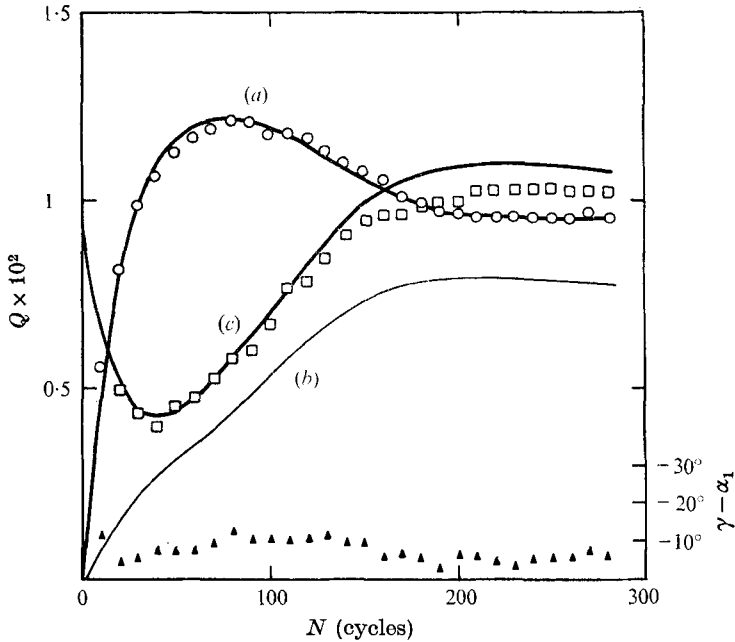


FIGURE 5. Evolution of an unstable interaction. Lines are solutions of equations (2.6): (a) 3/1 mode, (b) 2/1 mode, (c) 1/2 mode. Experiment:  $\circ$ , 3/1 mode;  $\square$ , 1/2 mode;  $\blacktriangle$ , 3/1 mode phase relative to paddle ( $\gamma - \alpha_1$ ). For the experiment,  $F/T_1 a_c \approx 1.39$ ;  $R_1 = 7.23 \times 10^5$ .

### 6.3. Spontaneous selection of the most unstable triad

It was indeed fortunate that the 2/1 and 5/1 mode triads listed in table 1 were discovered, for these provided a means of verifying the predictions of §4. For both modes (when  $L$  is  $3.10H$ ), the critical amplitude for the triad containing as another partner a free mode with  $N = 2$  happens to be greater than for one of the other triads. By initial forcing of the 3/2 free mode at the appropriate frequency using the movable wave maker, initial instability of the interacting triads (2/1, 1/3, 3/2)\*† could be predisposed. The test of the theory was whether the triad (2/1, 3/4, 5/5) would appear spontaneously and dominate the (2/1, 1/3, 3/2) interaction.

Figure 6(b) (plate 1) is a copy of the thermistor bridge record for a forced 2/1 mode superimposed upon a previously forced 3/2 mode. The probe was located at a position ( $0.555L$ ,  $\frac{1}{2}B$ ,  $\frac{11}{12}H$ ). The 3/2 forcing was ceased at moment  $A$  on figure 6(b) and supercritical forcing ( $F/a_c T_1 = 2.56$ ,  $F/a_c^* T_1 = 1.12$ ) of the 2/1 mode was commenced at  $B$ . The beating period of the 3/2 mode with the 2/1 mode is 5.06 cycles, which shows plainly on the record. After about 90 cycles, however, there is a detectable change in the modulation, another component of period 2.32 cycles appearing, then growing rapidly. After some time the strong persistent modulation has as its most recognizable components one with this period, and one of period 7.7 cycles. These periods correspond closely with the 2/1 mode, 3/4 mode beating period (2.31 cycles/cycle) and the 2/1 mode,

† An asterisk denotes the triad with the higher critical amplitude  $a_c^*$ .

( $5/5-3/4$ ) mode period [ $0.542/(0.307 - 0.235) = 7.55$  cycles/cycle]. The 5.06 period may still have been present, but it could not be distinguished.

A more rigorous test can be similarly applied in the case of the ( $5/1, 1/1, 4/2$ )\* and ( $5/1, 3/3, 8/4$ ) triads, whose critical amplitudes are much closer to one another than are those of the  $2/1$  triads. The experiment is more difficult, however, because (i) frequencies of the free modes of each are identical and (ii) there are no  $1/1$  nodal points at which the probe may be located to detect the growing  $3/3$  mode.

After the  $4/2$  mode had been forced, a supercritical forcing of the  $5/1$  mode ( $F/a_c T_1 \simeq 4.1$ ,  $F/a_c^* T_1 \simeq 3.5$ ) was applied. Figure 6(c) (plate 1) shows the thermistor record. The observed initial modulation is compounded from the beating of the  $5/1$  and  $4/2$  modes (2.77 cycles/cycle) and the  $5/1$  mode, ( $4/2 - 1/1$ ) mode beating period (3.62 cycles/cycle). The same modulation persisted over the whole experiment (1200 cycles of forcing). Primary de-energization of the forced mode by  $1/1$  mode,  $4/2$  mode interaction is shown by the decrease in amplitude after time (ii) on figure 6(c), and  $8/4$  modes, revealed by shadowgraphs and dyed layers in the liquid, were visibly present after time (iii), though over the duration of the record shown in the figure, the  $4/2$  mode had not entirely vanished. Figure 7(a) (plate 2) shows the shadowgraph at time (i), before the  $5/1$  mode was forced, and figure 7(b) (plate 2) was taken after 430 cycles.

Though the initial conditions were not exactly matched, this experiment showed all the major features of the numerical calculation presented in figure 1.

## 7. Conclusion

It has been shown here that for a linearly damped, resonantly interacting triad of waves, the highest frequency member of which is continuously forced, a stable limit state may be attained if the forcing is exactly in phase. The state is then as follows.

(i) The forced wave settles to a *critical amplitude* defined only by the damping coefficients of the other two waves, and by the coefficients of interaction of these waves with the forced wave.

(ii) If the forcing rate exceeds that required for this amplitude to be attained, all the excess power is used to energize the other two waves, each of which also attains a similarly defined limit state.

(iii) In the context of internal waves, the possible interacting triads may be numerous. If two or more triads are simultaneously close to satisfying resonance conditions, the stable limit state is one in which the forced wave falls to the lowest *critical amplitude* defined for the triads present. Before attaining this state, members of each triad continue to grow only so long as the forced wave amplitude exceeds the critical amplitude for that triad.

(iv) Regardless of the initial magnitudes of all waves present, the only ones remaining in the limit state are members of the triad with the lowest critical amplitude.

There exists in addition an unstable limit state in which only the forced mode is present; this requires all other members of possible resonant triads to be

completely absent. The possibility that there exist, in addition, stable limit *cycles* of energy exchange between triad partners has not been eliminated, but none were identifiable from numerical integrations of the interaction equations. During evolution of an unstable interaction, the relative phases of the waves approach their limit values more rapidly than the amplitudes. A quasi-steady state is therefore possible if the phase of the forcing varies slowly in time.

These results have been substantially confirmed by standing-wave experiments, and have some generality. In less well controlled situations, however, modifications may be required. For example, the triad partners of a forced wave may themselves be members of other resonant triads, and energy may cascade to these triads. Cascades of this type will always be towards lower frequencies. If the waves become large enough, forced interactions between them will become sources of shorter wavelength disturbance to the medium. This is felt to be one cause of the 'traumata' described in I.

For conditions of the present experiments resonant geometries are dense (q.v. table 1) and the comparative insensitivity of the resonant frequency sum (equation (A 7)) to  $L/H$  suggests that resonance is arbitrarily close with any forced mode. However, there is room for further work on the behaviour of damped interacting systems when detuned from resonance.

One of us (DWM.) gratefully acknowledges the support of a Monash Graduate Scholarship during the course of this work.

## Appendix. Derivation of the interaction equations

The Boussinesq equations for motions of a stratified liquid are

$$\nabla \cdot \mathbf{u} = 0, \quad (\text{A } 1)$$

$$\frac{\partial}{\partial t} \mathbf{u} + \frac{1}{\rho_0} \nabla p - \sigma \hat{\mathbf{z}} = -\mathbf{u} \cdot \nabla \mathbf{u} + \nu \nabla^2 \mathbf{u} + \mathbf{F}, \quad (\text{A } 2)$$

$$\partial \sigma / \partial t + \Omega^2 \mathbf{u} \cdot \hat{\mathbf{z}} = -\mathbf{u} \cdot \nabla \sigma, \quad (\text{A } 3)$$

where  $\mathbf{u}$ ,  $p$ ,  $\sigma = g(\rho_0 - \rho)/\rho_0$ ,  $\rho$  and  $\rho_0$  are the velocity, pressure, buoyancy acceleration, density and undisturbed density respectively,  $\Omega^2 = -g\rho_0^{-1}d\rho_0/dz$  is the square of the Brunt-Väisälä frequency of the liquid (assumed here to be constant),  $\hat{\mathbf{z}}$  is a unit vector in the vertical ( $z$ ) direction,  $F$  is a body force and  $\nu$  is the coefficient of viscosity. The diffusion of density (i.e. buoyancy) in (A 3) is neglected; this conforms with the conditions of the experiments as the diffusivity of salt in water is small compared with that of momentum.

In two-dimensional motion, the velocity may be expressed in terms of a stream function  $\psi$  such that  $\mathbf{u} = (\psi_x, 0, -\psi_x)$  and  $\text{curl } \mathbf{u} = (0, +\nabla^2 \psi, 0)$ . Rectangular co-ordinates are assumed with  $\hat{\mathbf{z}} \equiv (0, 0, 1)$  vertical. With the scaling

$$t = \Omega^{-1}t', \quad \psi = \Lambda^{\frac{1}{2}} H^{\frac{3}{2}} \psi', \quad \mathbf{x} = H \mathbf{x}', \quad \sigma = (\Lambda^{\frac{1}{2}} H^{\frac{1}{2}} \Omega) \sigma', \quad \mathbf{F} = \Lambda \mathbf{F}'$$

the equation  $\partial[\text{curl (A 2)}]/\partial t + \partial(\text{A 3})/\partial x$  takes the form, dropping primes,

$$\mathcal{L}[\psi'] \equiv \frac{\partial^2}{\partial t'^2} \nabla^2 \psi' + \frac{\partial^2 \psi'}{\partial x'^2} = \epsilon \left( \frac{\partial}{\partial t'} J[\psi', \nabla^2 \psi'] - \frac{\partial}{\partial x'} J[\psi', \sigma'] + \frac{1}{Re} \nabla^4 \left( \frac{\partial \psi'}{\partial t'} \right) - \nabla \mathbf{F}'_t \right), \quad (\text{A } 4)$$

where  $R = \Omega^2 H/\nu$ , and  $\epsilon = \Lambda^{\frac{1}{2}} H^{\frac{1}{2}}/\Omega^2$  is a measure of the nonlinear, viscous and forcing terms assuming that  $R\epsilon \sim 1$ .

The boundary conditions consistent with a rectangular closed tank are†

$$\left. \begin{aligned} \psi_x &= 0 & \text{at } z &= 0, 1, \\ \psi_z &= 0 & \text{at } x &= 0, L/H. \end{aligned} \right\} \tag{A 5}$$

If  $\epsilon \ll 1$ , assume that  $\psi = \psi_0 + \epsilon\psi_1 + \dots$  and  $\sigma = \sigma_0 + \epsilon\sigma_1 + \dots$ . Clearly  $\psi_0$  satisfies  $\mathcal{L}[\psi_0] = 0$ , and solutions satisfying the boundary conditions (A 5) have the form  $\psi_0 = a \sin mx \sin nz \cos(\omega t + \alpha)$ , where  $a$  and  $\alpha$  are constants,  $m = M\pi/L$ ,  $n = N\pi/H$ , where  $M$  and  $N$  integers, and  $\omega^2 = M^2/(M^2 + N^2 L^2/H^2)$ .

If three waves exist,

$$\psi_0 = \sum_{j=1}^3 a_j \sin m_j x \sin n_j z \cos(\omega_j t + \alpha_j), \tag{A 6}$$

and if

$$\Sigma m_j = \Sigma n_j = \Sigma \omega_j = 0 \tag{A 7}$$

and the wave with  $j = 1$  is forced at a resonance of the container, then substitution of (A 6) into the equation for  $\psi_1$  gives rise to secular terms. These may be removed by assuming  $a_j$  and  $\alpha_j$  to be functions of the ‘slow’ time variable  $T = \epsilon t$  and subsequently treating  $T$  and  $t$  as independent.‡ The operator  $\partial/\partial t$  becomes  $\partial/\partial t + \epsilon\partial/\partial T$  and  $\psi_1$  satisfies

$$\begin{aligned} \mathcal{L}[\psi_1] = & -2 \frac{\partial}{\partial T} \nabla^2 \frac{\partial \psi_0}{\partial t} + \frac{\partial}{\partial t} J[\psi_0, \nabla^2 \psi_0] - \frac{\partial}{\partial x} J[\psi_0, \sigma_0] - \frac{1}{R\epsilon} \nabla^4 \frac{\partial \psi_0}{\partial t} \\ & + F^* \sin m_1 x \sin n_1 z \sin\{\omega_1 t + \gamma(T)\}, \end{aligned} \tag{A 8}$$

where

$$F^* = \sum_N \frac{H\omega^4(m^2 + n^2) a_N (-1)^N n}{\epsilon 2\Omega^6 m^3 L}.$$

The conditions for no secular terms to occur in (A 8) determine  $a_j(T)$  and  $\alpha_j(T)$ . In dimensional terms, these are precisely equations (2.1)–(2.6).§

† The introduction of forcing through the boundary conditions in I is replaced here by a body force

$$\mathbf{F} = \Sigma (-1)^M \frac{a_N n 2\omega^3}{m^3 L \Omega^2} \cos \omega t (n \sin mx \cos nz, 0, -m \cos mx \sin nz),$$

where  $a_N = 0$  for  $N$  even and  $-4A\omega H/(\pi^2 N^2)$  for  $N$  odd, which is formally equivalent.

‡ This is the method of two-timing; see, for example, Cole (1968, chap. 3).

§ These equations should be compared with the corresponding equations (B 14) of Martin, Simmons & Wunsch (1972), which apply to unforced and undamped progressive waves. McIntyre (private communication) has pointed out that space differentiations on the right-hand side of their equation (B 5) can introduce phase shifts of  $90^\circ$  for progressive waves but not for standing waves and that this fact explains the reversed positions of  $\cos \eta$  and  $\sin \eta$  between our theory and theirs.

## REFERENCES

- BALL, F. K. 1964 Energy transfer between external and internal waves. *J. Fluid Mech.* **19**, 465–480.
- COLE, J. D. 1968 *Perturbation Methods in Applied Mathematics*. Blaisdell.
- CRAIK, A. D. D. 1971 Nonlinear resonant instability in boundary layers. *J. Fluid Mech.* **50**, 393–413.
- DAVIS, R. E. & ACRIVOS, A. 1967 The stability of oscillatory internal waves. *J. Fluid Mech.* **30**, 723–36.
- HASSELMANN, K. 1966 Feynman diagrams and interaction rules of wave–wave scattering processes. *Rev. Geophys.* **4**, 1–32.
- HASSELMANN, K. 1967 A criterion for nonlinear wave stability. *J. Fluid Mech.* **30**, 737–39.
- MC EWAN, A. D. 1971 Degeneration of resonantly-excited internal gravity waves. *J. Fluid Mech.* **50**, 431–48.
- MCGOLDRICK, L. F. 1965 Resonant interactions among capillary–gravity waves. *J. Fluid Mech.* **21**, 305–31.
- MCGOLDRICK, L. F. 1970 An experiment on second-order capillary–gravity resonant wave interactions. *J. Fluid Mech.* **40**, 251–71.
- MARTIN, S., SIMMONS, W. & WUNSCH, C. 1972 The excitation of resonant triads by single internal waves. *J. Fluid Mech.* **53**, 17–44.
- PHILLIPS, O. M. 1966 *The Dynamics of the Upper Ocean*. Cambridge University Press.

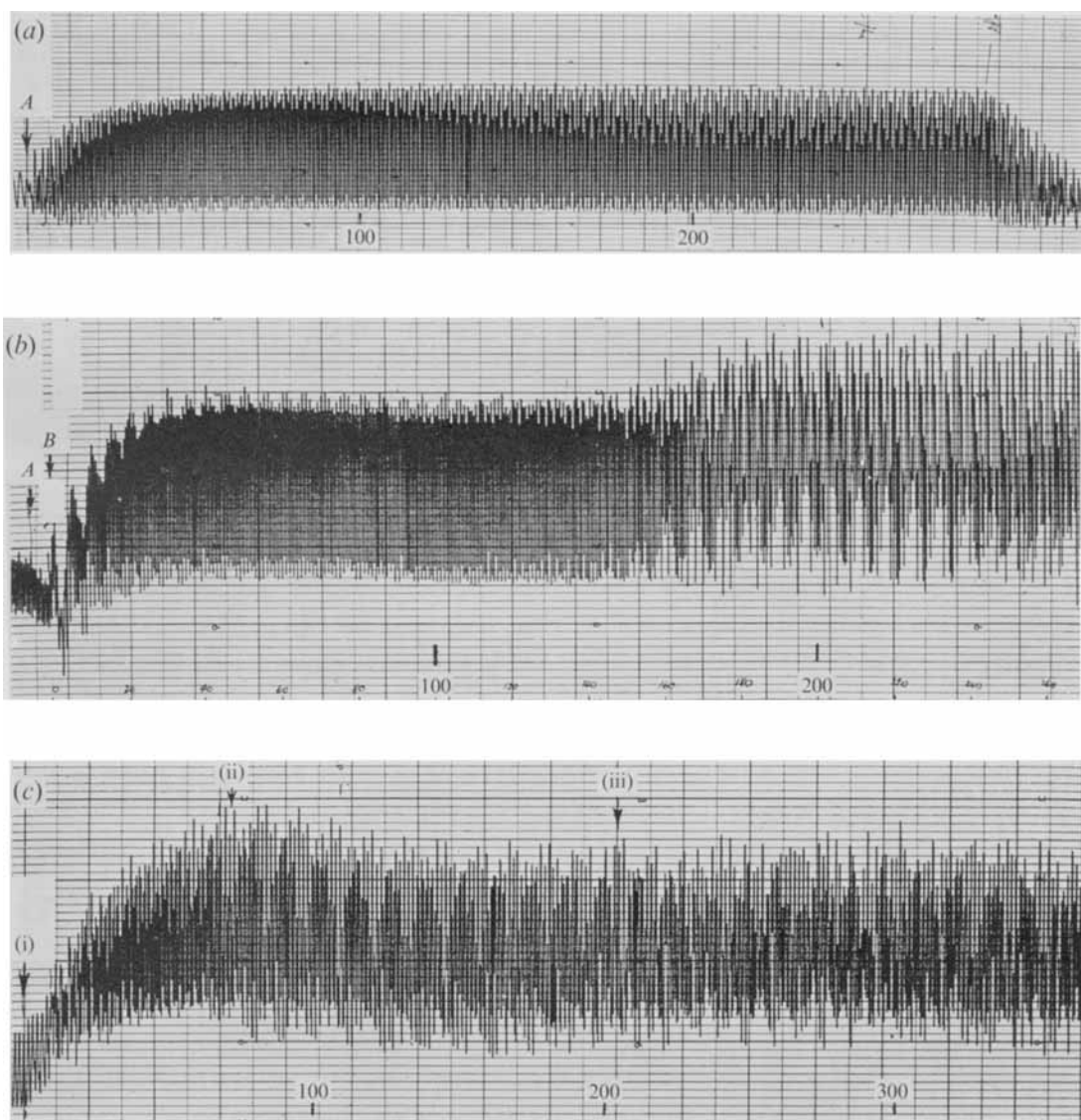
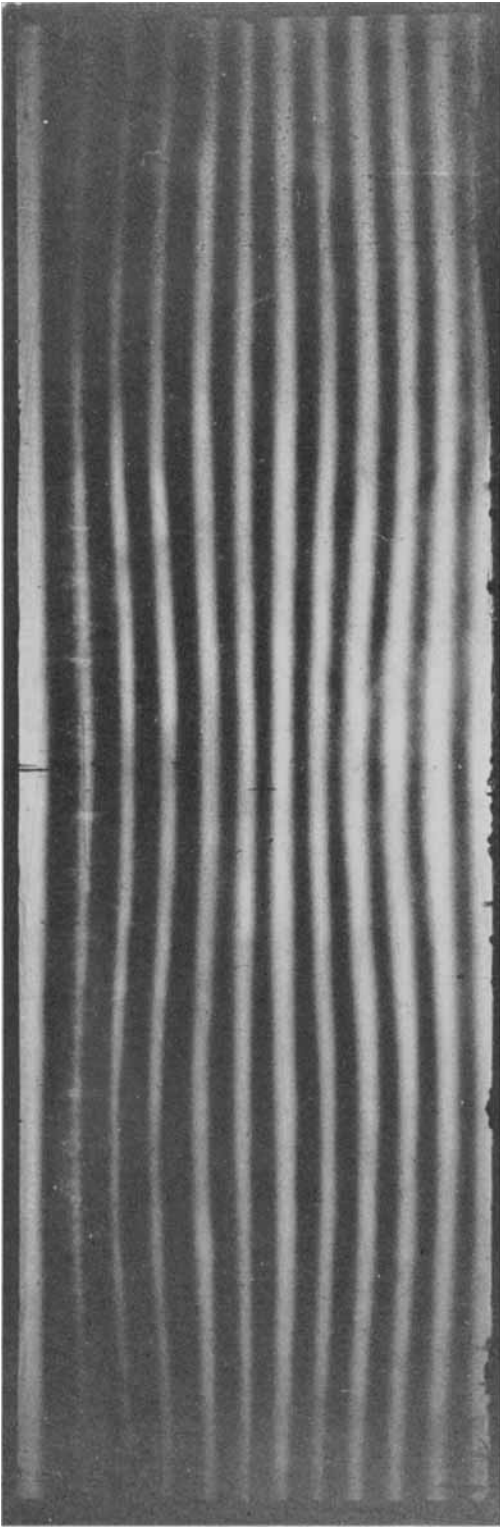
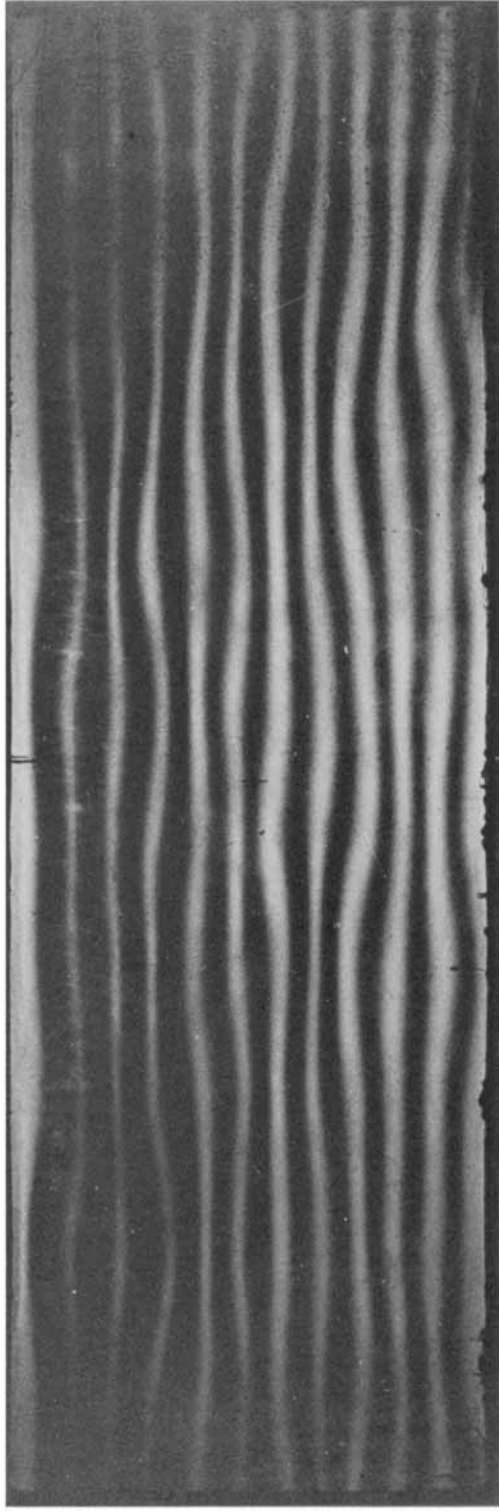


FIGURE 6. Recorder traces from thermistor bridge, showing modulation by interacting free modes. (a) Record providing results given in figure 4. Initial imposed  $1/2$  wave was discontinued at *A*, when forcing of  $3/1$  mode was commenced. (b) Spontaneous growth of  $3/4$ ,  $5/5$  modes upon a previously imposed  $(2/1, 1/3, 3/2)$  triad interaction. (c) Spontaneous growth of the  $3/3$  and  $8/4$  modes upon a previously imposed  $(5/1, 1/1, 4/2)$  triad interaction. See also figures 1 and 7.



(a)



(b)

FIGURE 7. Shadowgraphs of dyed layers, 5/1 mode resonant forcing. (a) At time (i) on figure 5 (c), 4/2 mode only present. (b) After 430 cycles.